

Hemoglobin degradation in human erythrocytes with long-duration near-infrared laser exposure in Raman optical tweezers

Raktim Dasgupta
Sunita Ahlawat
Ravi Shanker Verma
Abha Uppal
Pradeep Kumar Gupta

Raja Ramanna Centre for Advanced Technology
Laser Biomedical Applications and Instrumentation
Division
Indore 452013, India

Abstract. Near-infrared laser (785-nm)-excited Raman spectra from a red blood cell, optically trapped using the same laser beam, show significant changes as a function of trapping duration even at trapping power level of a few milliwatts. These changes in the Raman spectra and the bright-field images of the trapped cell, which show a gradual accumulation of the cell mass at the trap focus, suggest photoinduced aggregation of intracellular heme. The possible role of photoinduced protein denaturation and hemichrome formation in the observed aggregation of heme is discussed. © 2010 Society of Photo-Optical Instrumentation Engineers. [DOI: 10.1117/1.3497048]

Keywords: Raman spectroscopy; optical tweezers; red blood cells; hemoglobin.

Paper 10065R received Feb. 9, 2010; revised manuscript received Aug. 10, 2010; accepted for publication Aug. 25, 2010; published online Oct. 5, 2010.

1 Introduction

The increasing interest in the use of Raman spectroscopy for studies of the chemical composition and conformation of macromolecules in individual cells stems from the fact that this technique avoids the necessity of any exogenous stain. However, due to the inherent weak nature of the Raman signal, a long acquisition time (often tens of seconds to few minutes) is required^{1,2} to acquire spectra with a good SNR. The cell should therefore be immobilized. But the physical or chemical methods used for immobilization of cells in micro-Raman techniques often lead to undesirable surface-induced effects on the cells or lead to strong background spectra originating from the substrate/immersion medium.^{3,4} The use of radiation forces⁵ exerted by a tightly focused optical beam to immobilize cell without direct contact helps to avoid these problems and therefore Raman optical tweezers³ or a setup facilitating acquisition of Raman spectra from an optically trapped cell, are receiving much attention. In particular the use of near-IR radiation for Raman studies is gaining rapid interest due to much reduced fluorescence background that often obscures the small but important Raman bands. The near-IR (NIR) Raman optical tweezers have already been utilized for several interesting studies such as monitoring the real-time heat denaturation of yeast cells,⁶ the transition from the oxygenated to deoxygenated condition of a red blood cell (RBC) on application of mechanical stress,⁷ sorting and identification of microorganisms,⁸ etc. Note here that Raman spectroscopy is a powerful technique to monitor the oxygen-carrying capacity of RBCs since the binding or the dissociation of oxygen with heme leads to significant conformational changes that can be sensitively monitored by this technique. However, since optical trapping of cells requires

the use of high-numerical-aperture (NA) lenses (typically $NA > 1.2$), even at a trap power level of few milliwatts, the intensity at the sample is very high ($\sim MW\text{ cm}^{-2}$). Therefore, the possibility of photoinduced damage to the trapped cells must be carefully examined. Previous studies on Raman spectroscopy of RBCs utilizing Ar:Kr ions,^{9,10} He-Ne (Ref. 11), and NIR (Ref. 12) lasers to excite Raman spectra have shown significant photoinduced damage for long exposure times. With a power of $\sim 0.75\text{ mW}$ (irradiance at the sample $\sim 80\text{ kW cm}^{-2}$) at Ar:Kr ion laser lines (488, 514, and 568.2 nm) used to excite Raman spectra, significant changes in the Raman spectra acquired from RBC trapped using a 830-nm laser beam were observed as a function of time.⁹ These changes were attributed to the formation of methemoglobin (met-Hb) due to photoinduced irreversible binding of oxygen to the heme groups. However, note that in the studies carried out by Ramser et al.,⁹ the resonant absorption of the laser wavelengths by met-Hb led to a high-fluorescence background, which may obscure observation of small changes that may be crucial for understanding the role of other possible pathways of photoinduced damages. Micro-Raman studies¹¹ carried out by Wood et al. using a He-Ne laser beam (632.8 nm, irradiance $\sim 113\text{ kW cm}^{-2}$) also showed significant changes in the spectra as a function of the exposure time. The observation that these changes were similar to that observed in Raman spectra of an RBC acquired at elevated temperature led them to suggest that the laser-exposure-induced changes may arise due to hemoglobin (Hb) aggregate formation resulting from photoinduced protein denaturation. Though in the study carried out by Ramser et al.,⁹ no photo-damage was observed in cells trapped for duration of up to 10 min by NIR trapping laser light (830 nm, irradiance $\sim 13\text{ MW cm}^{-2}$), in the study carried out by Wood et al.¹² using 785-nm excitation, significant damage above 18 mW

Address all correspondence to: Raktim Dasgupta, Raja Ramanna Centre for Advanced Technology, Laser Biomedical Applications and Instrumentation Division, Indore-452013, India. Tel: 917-312-488-427; Fax: 917-312-488-425; E-mail: raktim@rrcat.gov.in

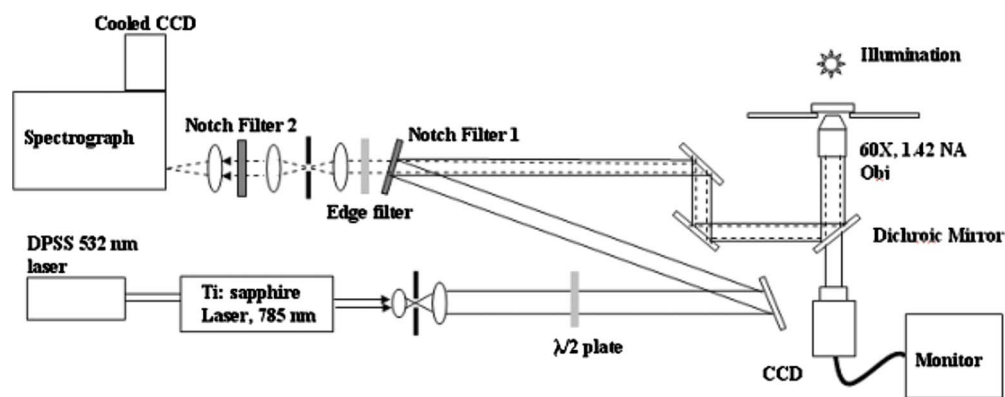


Fig. 1 Experimental setup. The solid line shows the trapping/excitation beam, whereas the dotted line indicates the Raman signal.

(irradiance $\sim 1 \text{ MW cm}^{-2}$) for exposure durations $\sim 200 \text{ s}$ was observed. In this study, the RBCs were fixed onto the glass substrate using poly-L-lysine, which may also lead to unwanted surface-induced effects and may also hinder observation of early stage of photodamage.⁴

We therefore studied photoinduced changes in RBCs as a function of the duration of laser exposure in Raman optical tweezers employing an NIR (785-nm) laser source. The use of Raman optical tweezers helped in the acquisition of good quality spectra by manipulating the trapped cell away from the surface, thereby minimizing unwanted background originating mostly from the substrate and immersion medium. Further fluorescence coming from the trapped RBC itself, which may suppress the small spectral alterations present at early stages of photodamage, was minimized by using NIR excitation. The changes observed in the Raman spectra and bright-field images as a function of exposure time suggest initiation of aggregation of hemoglobin in the trapped RBC at a much lower exposure value than reported previously. The spectral changes suggest simultaneous occurrence of protein denaturation and hemichrome formation. The possible involvement of nonlinear light absorption effect in the observed photoinduced changes in the cells is also discussed.

2 Materials and Methods

Figure 1 shows a schematic of the experimental setup. The 785-nm cw beam from a Ti:sapphire laser (Mira 900, Coherent Inc.), pumped by a 532-nm diode-pumped solid state laser (Verdi-5, Coherent Inc.), was chosen for both trapping and exciting the Raman signal. The laser beam was filtered to obtain a smooth profile and then introduced into a homebuilt inverted microscope equipped with a high-NA objective lens (Olympus 60 \times , NA 1.42), forming an optical trap. For trapping and acquisition of Raman spectra we used laser powers varying from 3 to 9 mW, measured at the specimen plane. The laser spot size at the focus was $\sim 0.5 \mu\text{m}$ and the RBCs were trapped $\sim 15 \mu\text{m}$ above the bottom cover plate of the sample holder. A holographic notch filter (notch filter 1), was used to reflect the 785-nm trapping/excitation beam at an incident angle of $\sim 12 \text{ deg}$. The Raman signal backscattered from the trapped RBC was collimated by the objective lens and passed back along the same optical pathway. Notch filter 1 transmits the Raman signals above

800 nm, which are then passed through a $100\text{-}\mu\text{m}$ confocal pinhole to reject most of the off-focus Rayleigh scattered laser light. It was thereafter passed through another notch filter (notch filter 2) that further removes the Rayleigh scattered laser light. The beam was then focused onto the entrance slit of an imaging spectrograph (Shamrock SR-303i, Andor Corp.). The spectrograph is equipped with 600-lines/mm and 1200-lines/mm gratings blazed at a wavelength of 900 nm and incorporates a back-illuminated CCD (iDus DU420-BR-DD, Andor Corp.) camera thermoelectrically cooled to $-80 \text{ }^\circ\text{C}$. To allow observation of the trapped RBCs a green-filtered halogen illumination source and a video CCD camera system were used.

Calibration of the spectrometer was performed using toluene (Spectroscopic grade, Aldrich) and assignment of the peaks was made from standard spectra. The spectral resolution of the Raman system was about 4 cm^{-1} with a 1200-lines/mm grating and the Raman spectra can be recorded in the range from ~ 950 to $\sim 1600 \text{ cm}^{-1}$. The resolution with a 600-lines/mm grating was $\sim 6 \text{ cm}^{-1}$, but spectra could be recorded over a region of ~ 500 to 2100 cm^{-1} region. We recorded spectra without a cell in the trap and then subtracted this background spectra from the Raman spectra acquired from the trapped RBC to remove the background arising from the buffer, substrate, and objective immersion oil.^{6,15}

The absorption spectra of met-Hb, hemichrome, and oxy-hemoglobin (oxy-Hb) were monitored over ~ 400 to 900 nm using a Cintra 20 (GBC, Australia) UV-visible spectrometer. The measurement parameters were set to a 1-mm slit width, 500 nm/min scan speed, and data were recorded at $\sim 1\text{-nm}$ intervals. About 2 ml of samples were placed in a quartz cuvette, while another quartz cuvette filled with 1.5 mM phosphate buffer served as background.

Blood (1 ml) was collected by venipuncture from healthy volunteers in glass tubes containing EDTA (5.4 mg/3 ml) as an anticoagulant. RBCs were separated from these anticoagulated blood samples by centrifugation at 3000 rpm for 3 min. The separated RBCs were then washed with phosphate buffer saline (PBS) and suspended in 1.5 mM phosphate buffer containing 290 mM sucrose. This buffer maintains the osmolarity of the suspending media and inhibits the adherence of cells to glass surface.¹⁴ Appropriate dilutions of the cells in buffer

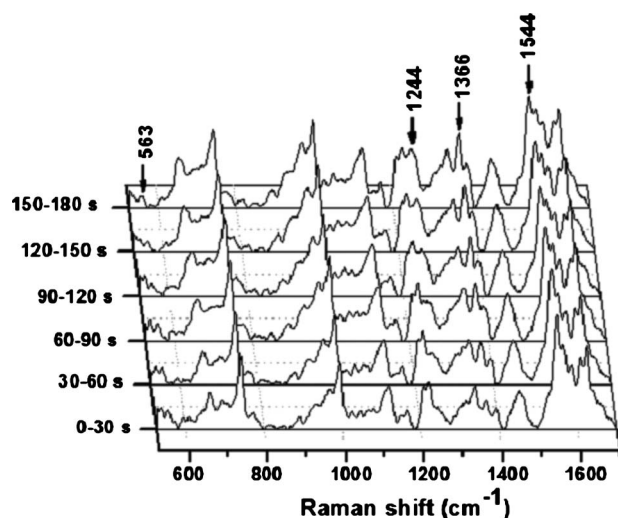


Fig. 2 Temporal evolution of Raman spectra observed from trapped RBCs with trapping/excitation laser power of ~ 7 mW, recorded over a 525- to 1700- cm^{-1} region using a 600-lines/mm grating. The spectra shown are the mean of three cells. Iterative polynomial fitting was applied to the baseline to remove the background. The Raman bands showing temporal change in intensity are indicated.

solution were then used for experiments. For experiments with RBCs containing met-Hb the washed RBCs were resuspended in 0.1% sodium nitrate solution and the suspension was allowed to stand for ~ 1 h at room temperature.¹¹ The cells were thereafter washed in PBS and resuspended in the same buffer. Oxy-Hb solution was prepared following method described in Ref. 15. For preparation of hemichrome solution, the method described in Ref. 16 was used. The formation of met-Hb and hemichrome was confirmed from UV-visible spectroscopy showing marker band at ~ 635 and ~ 537 nm for met-Hb and hemichrome, respectively.¹⁶

3 Results and Discussion

To study the effect of laser exposure on RBCs held in Raman optical tweezers, first we acquired consecutive time-lapsed Raman spectra in the wave number region of 525 to 1700 cm^{-1} with an acquisition time of 30-s for each spectra over a total time period of 3 min. The results are shown in Fig. 2. The trapping/excitation power used was ~ 7 mW and for exposure time of a few tens of seconds significant changes could be seen for the Raman bands at 1244, 1366, and 1544 cm^{-1} along with a small decrease in intensity of the band at 563 cm^{-1} and a gradual increase in SNR. As the spectral region above 1000 cm^{-1} undergoes most significant changes, we investigated this region in detail. Further, for improved statistical validation, spectra were recorded from blood samples collected from five healthy volunteers. For each blood sample, at least seven RBCs were studied. Figure 3(a) shows the Raman spectra acquired at time intervals of 0 to 5 and 175 to 180 s, from seven RBCs in the blood sample of a healthy donor. Significant time-dependent changes can be seen in all the spectra. Notably, when we apply no baseline fitting to the acquired spectra, there was also a significant difference in the baseline offset between the spectra collected at 0 to 5 and 175 to 180 s. Figure 3(b) shows the mean spec-

tra from five samples. The spectral changes with time are noted to be similar for RBCs collected from all the five blood samples.

To observe the effect of laser power on the time evolution of the spectra, the spectra were recorded at laser powers of ~ 5 , ~ 7 , and ~ 9 mW. Figure 4 shows the temporal evolution of the mean Raman spectra (recorded between 950 and 1600 cm^{-1}) from trapped RBCs, at room temperature (~ 25 °C). For clarity, spectra collected over only seven time intervals are shown as representative of the observed time lapse changes. The spectra collected at increasing exposure times show substantial baseline shift with time.

From Fig. 4 we can see that with increased exposure duration, the Raman spectra show change in many Raman bands. Notably most of the significant Raman bands observable in RBC spectra are contributed by intracellular hemoglobin as the cytoplasmic proteome in red blood cells is composed of 98% hemoglobin¹⁷ and therefore while acquiring Raman spectra of RBCs the signature of Hb supersedes all other proteins.^{11,12,18} The assignment (Table 1) for some important Raman bands follows from the work by Abe et al.¹⁹ and Wood et al.¹² Band assignments were considered for only oxygenated Hb as the cells were kept at equilibrium with atmospheric oxygen.

The bands in the region between 1500 and 1700 cm^{-1} are known to serve as spin state markers. The normal mode at 1544 cm^{-1} primarily consists of $\text{C}_\beta\text{-C}_\beta$ bond stretching and is sensitive to photooxidation of heme.¹⁸ The 1366- cm^{-1} band assigned to local coordinate ν_4 involve pyrrole half-ring stretching vibration and are known as oxidation state marker.^{18,20} The band at 1244 cm^{-1} is associated with C-H in plane vibrations of methine hydrogen in porphyrin macrocycle.^{18,20,21} The 563- cm^{-1} band comes from Fe- O_2 stretching and is indicative of oxygenation state of the central iron atom.²²

The observation of enhanced intensities of the 975-, 1244-, and 1366- cm^{-1} Raman bands is consistent with the previous report by Wood et al.¹¹ Since similar spectral changes were observed during thermal denaturation of Hb, they attributed these changes to the aggregation of heme moieties as a consequence of photoinduced denaturation of Hb. Further, the peak at 1544 cm^{-1} is resonantly enhanced with laser wavelength of 785 nm and the decrease in intensity of this peak can be ascribed to conversion of oxy-Hb to met-Hb, in which oxygen is irreversibly bound to heme, as indicated in previous studies.^{9,23} Note here that high-spin met-Hb is less stable than hemichrome, a low-spin component in which the sixth coordination site of the iron is occupied by the imidazole group of the distal histidine, and can be spontaneously converted to the latter.^{22,24} Additionally, any possible denaturation of intracellular Hb due to light damage action also helps the formation of hemichrome as disruption of globin structure facilitates the coordination of the imidazole group of the distal histidine with the iron atom.²² Therefore, we recorded met-Hb and hemichrome Raman spectra to correlate with the observed photoinduced changes. The spin marker bands in the spectral region ~ 1500 to 1600 cm^{-1} for met-RBC and hemichrome are shown in Figs. 5(a) and 5(b). The spectra shown in Figs. 5(a) and 5(b) were acquired with an excitation/trapping power of ~ 3 mW to ensure no photoinduced changes in the spectra.

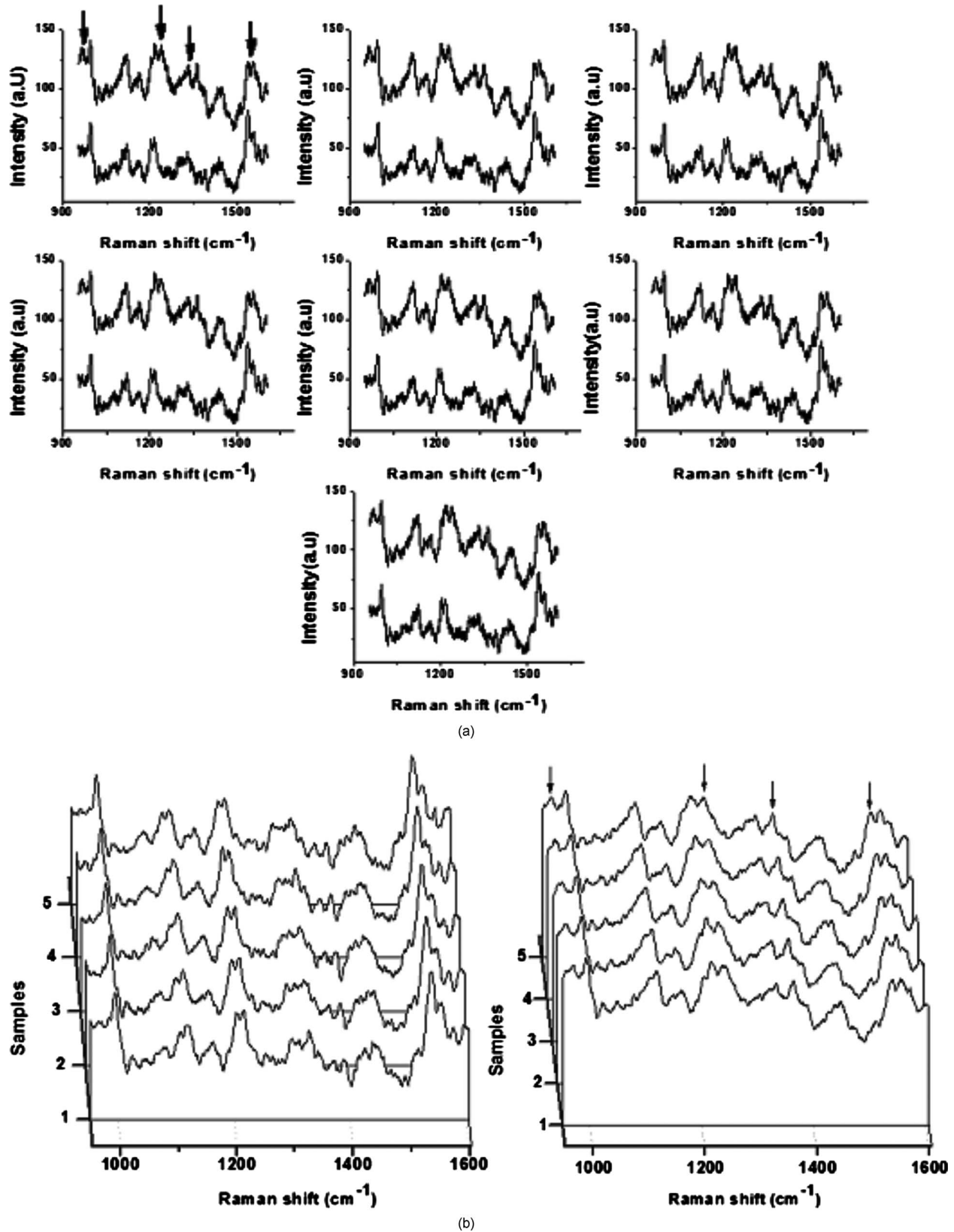


Fig. 3 (a) Raman spectra acquired from trapped RBCs at ~ 5 mW of trapping power. In each graph the bottom spectra are acquired at 0 to 5 s and top spectra are acquired at 175 to 180 s. The large baseline shift can be seen for spectra collected at the 175- 180-s interval. Further, several Raman peaks (indicated by arrows) located at 975, 1244, 1366, and 1544- cm^{-1} suffer significant change in intensity due to prolonged laser exposure. (b). Mean Raman spectra from five blood samples at 0 to 5 s (left) and 175 to 180 s (right). From each sample, spectra were acquired from \sim seven cells. The changes are indicated by arrows. All spectra were acquired with a 1200-lines/mm grating.

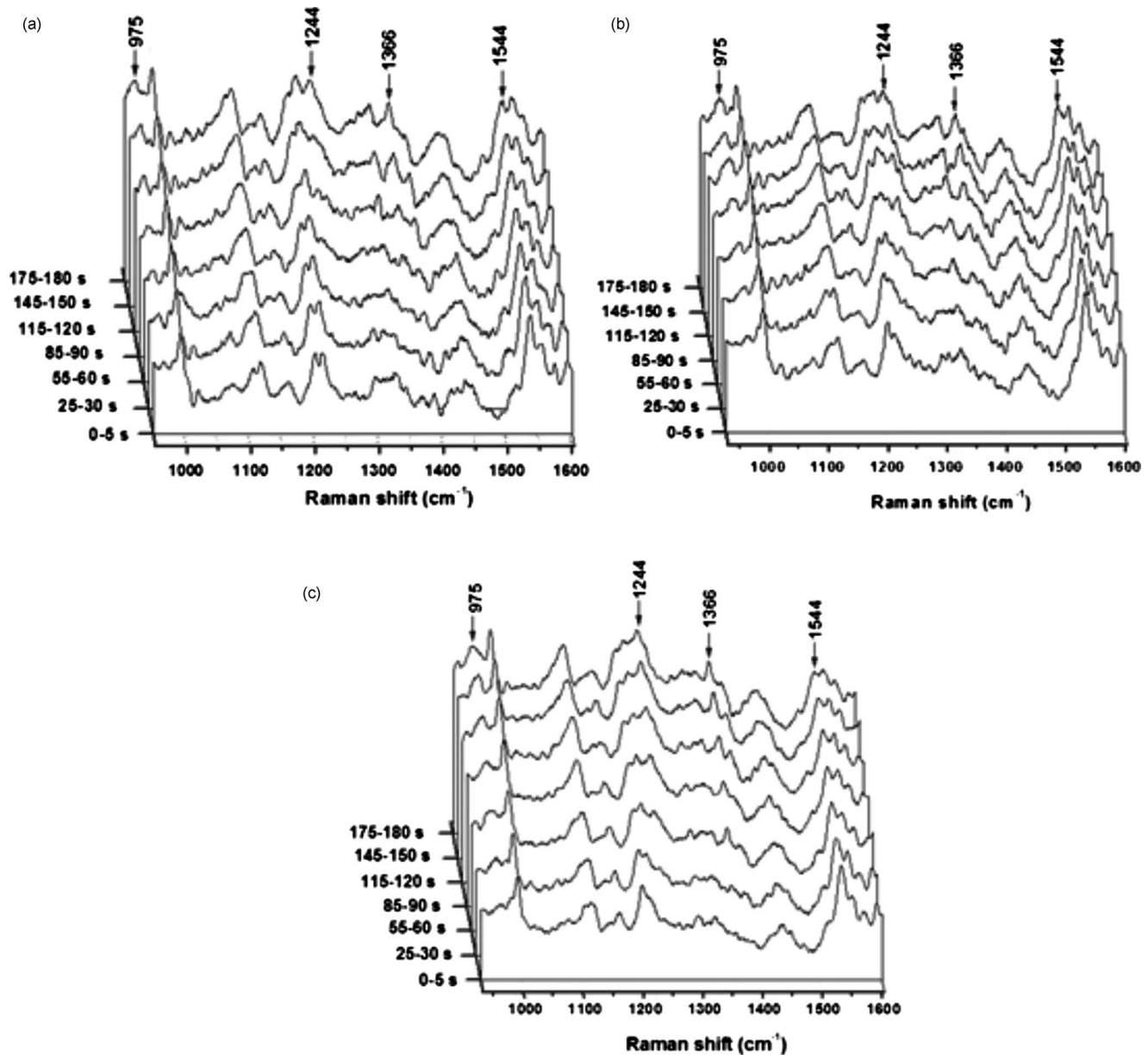


Fig. 4 Time evolution of Raman spectra observed from trapped RBCs with trapping/excitation laser power of (a) ~ 5 , (b) ~ 7 , and (c) ~ 9 mW. The corresponding irradiance at the specimen is (a) ~ 2.55 , (b) ~ 3.57 , and (c) ~ 4.58 MW cm^{-2} . The Raman bands showing temporal change in intensity are indicated.

The spectral changes noted for met-Hb and hemichrome when compared with photoinduced changes shown in Fig. 5(c), indicate predominant formation of hemichrome in the damaged cells. A reduction in the 563-cm^{-1} peak, as seen from spectra in Fig. 2, is also indicative of this above fact.²² Therefore, photoinduced degradation of Hb inside optically trapped RBCs may be an interplay of photoinduced denaturation of Hb as well as photooxidation affected hemichrome formation.

As the photodamage observed for RBCs due to laser exposure can be largely attributed to Hb denaturation phenomena, similar to what was observed¹¹ for heat-treated RBCs, it is important to investigate the possible role that the elevated temperature at the trap focus might play. The steady state temperature rise in optical trap has been estimated by Ramser

et al. to be less than 1 K, considering water as the prime absorber of laser power.⁹ However, note that as RBCs contain a very high concentration²⁵ of Hb (~ 5 mM) and the absorption coefficient of Hb at the NIR region is much higher than that of water, light absorption by intracellular Hb cannot be neglected for reasonable estimation of temperature increase. The temperature increase at the focus can be given as,²⁶

$$\Delta T = P \left(b \left[\ln \left(\frac{2\pi R}{\lambda} \right) - 1 \right] + db \left\{ \frac{\ln \left[(2\pi r_p / \lambda)^2 + 1 \right]}{2} \right\} \right), \quad (1)$$

where P is the trapping laser power, R is the distance of the focus from the cover glass surface, λ is the laser wavelength,

Table 1 Assignment and spectral position (in inverse centimeters) of the Hb Raman bands undergoing significant temporal intensity change, as shown in Fig. 4. For comparison bands observed by Wood et al.¹² for oxygenated Hb are also shown.

Band Assignment	Local Coordinates	Band Position (cm ⁻¹)	Band Position (cm ⁻¹) (Ref. 12)
ν_{11}	$\nu(\text{C}_\beta\text{C}_\beta)$	1544	1547
ν_4	$\nu(\text{pyr half-ring})_{\text{sym}}$	1366	1371
ν_{42}	$\delta(\text{C}_m\text{H})$	1244	1248
ν_{46}	$\delta(\text{pyr deform})_{\text{sym}}$ and/or $\gamma(\text{C}_6\text{H}_2)_{\text{sym}}$	975	974
$\nu(\text{Fe}-\text{O}_2)$	$\nu(\text{Fe}-\text{O}_2)$	563	567

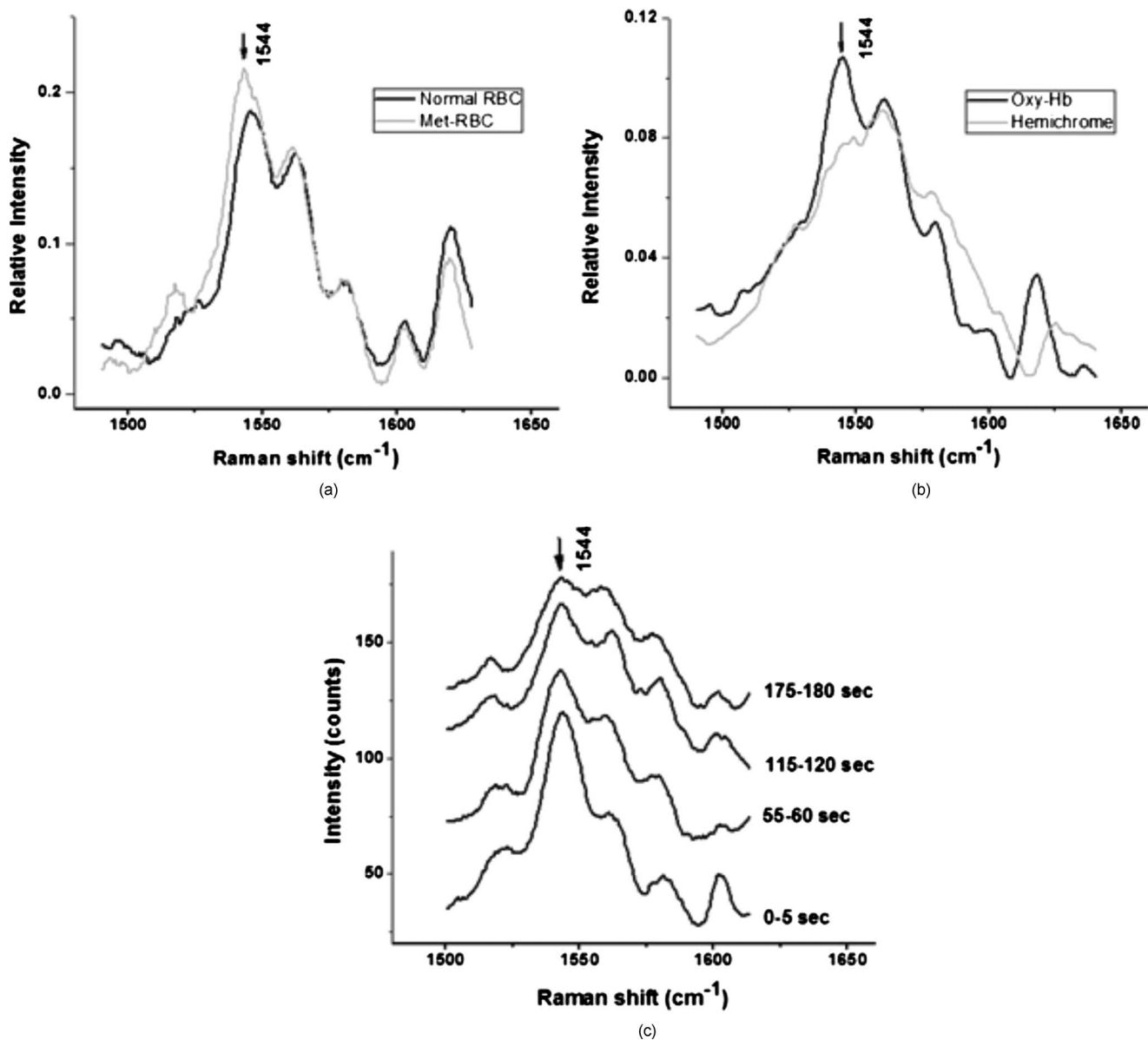


Fig. 5 (a) Raman spectra of RBC containing oxy-Hb and met-Hb. (b) Raman spectra from oxy-Hb solution and hemichrome solution. The spectra were recorded at an excitation/trapping power of ~ 3 mW over a recording time of ~ 30 s. Spectra shown are the mean from five acquisitions. (c). The time-lapse spectra from photodamaged RBCs at an excitation/trapping power of ~ 9 mW. The 1544-cm⁻¹ Raman peak is indicated by arrow.

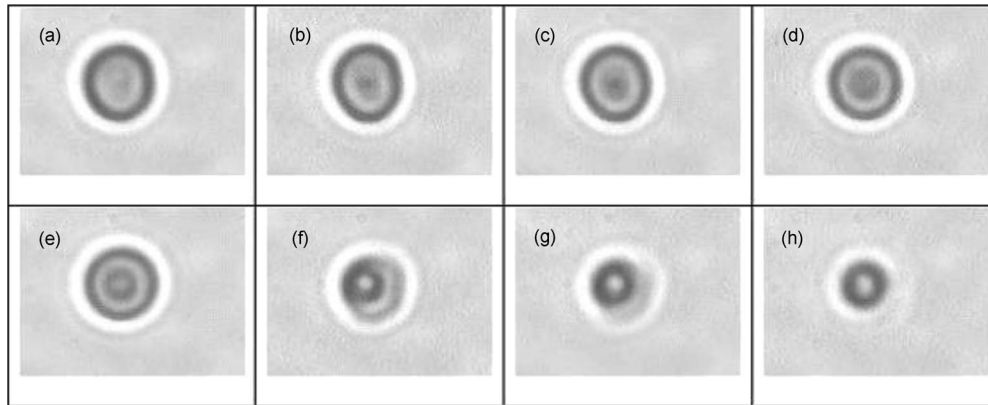


Fig. 6 Images of a trapped RBC with ~ 9 mW of laser power showing changing appearance of the cell, due to condensation of the cell mass at the trap focus, with duration of laser exposure of (a) 22, (b) 25, (c) 28, (d) 31, (e) 33, (f) 33.6, (g) 33.9, and (h) 36 s.

and r_p is the effective radius of the red blood cells. The coefficient b is defined as

$$b \equiv \frac{\alpha}{2\pi K}, \quad (2)$$

where α is the absorption coefficient, and K is the thermal conductivity of water. Note that db is the differential change of b for the RBCs with respect to water.

Taking the values as $\alpha_{\text{water}} \sim 3 \text{ m}^{-1}$ (Ref. 27), $K_{\text{water}} \sim 0.6 \text{ W/mK}$ (Ref. 26), $\alpha_{\text{Hb}} \sim 370 \text{ m}^{-1}$ (Ref. 28), $K_{\text{Hb}} \sim 0.45 \text{ W/mK}$ (Ref. 29), and the mean radius for the RBCs as $\sim 3 \mu\text{m}$, the temperature rise at the focus for laser power of 5 to 9 mW, was estimated to be between 2 to 3.7 K. As the experiments were performed at room temperature ($\sim 25^\circ\text{C}$), the elevated temperature at the focus was $< 29^\circ\text{C}$, not sufficient for causing heat denaturation to the cells.

The Raman spectra also show a marked increase in baseline and a gradually increasing intensity for all the Raman bands with laser exposure time. Wood et al. also observed the same effect and ascribed it to excitonic interaction mechanism between the metalloporphyrins resulting in migration of energy throughout the aggregated heme network.¹¹ However, intrinsic fluorescence coming from photogenerated hemichrome³⁰ may also contribute to the baseline enhancement. Therefore, we investigated the time evolution of the bright field images of the cell. Figure 6 shows time-separated images of a trapped cell at ~ 9 mW of laser power. Note here that RBCs were suspended in isotonic buffer so that they maintained their natural biconcave shape. Though the equilibrium orientation of the biconcave RBC under optical trap is side-on type,^{31–33} we observed that for small trapping power (< 10 mW) used in our studies the cells can be captured by optical forces but they do not turnover. This is possibly caused by the small gradient force that resulted in our case, which is unable to generate sufficient torsional moment required to turnover the cells.³⁴

As we can see from bright-field images of the trapped cell in Fig. 6, the change in density of the cytoplasmic mass starts at the center, and gradually the entire cell is affected and the majority of the cell mass becomes densely packed at the trap

focus. A plausible explanation for this observation is that in an optically trapped RBC, the precipitated heme, resulting from protein denaturation and photooxidation, is attracted toward the trap focus, and this may lead to the formation of heme aggregate at the trap focus. We also checked the effect of relaxation on the cells when they were released from the trap after 36 s. Monitoring the cell for ~ 10 min showed no sign of it regaining its normal physiology, and therefore we could conclude that the laser-induced effects were not reversible.

Fig 7 shows the time evolution of the intensity of Raman bands at 975, 1244, 1366, and 1544 cm^{-1} , relative to the baseline. As the peak intensities are influenced significantly by adjacent Raman bands, to estimate the actual intensities of the Raman peaks, Lorentzian fitting was performed that can effectively minimize the error contributed by overlapping regions of adjacent bands. Also, the temporal change in baseline offset of the spectra and mean Raman signal amplitude are shown. The mean Raman amplitudes were estimated over other Raman peaks [996 (ν_{45}), 1170 (ν_{30}), 1210 ($\nu_5 + \nu_{18}$), 1434 (ν_{28}), and 1551 cm^{-1} (ν_{11})] that do not show significant temporal variation. We can see that for peaks at 975, 1244, and 1366 cm^{-1} , initially the intensity increases slowly until a particular point of time is reached, where a steep increase in intensity could be noted. The time intervals at which the steep increases in intensity could be seen are 90 to 100, 50 to 60, and 30 to 40 s for excitation powers of ~ 5 , ~ 7 , and ~ 9 mW, respectively. The similar time variation patterns of these Raman bands can be understood by considering their primary association with photoinduced denaturation of Hb inside RBC. The rapid intensity variation of the Raman bands associated with photodenaturation at specific time intervals is also in quantitative agreement with the microscopy data presented in Fig. 6, which show that the rate of dense packing of erythrocyte cell mass rises sharply at ~ 33 to 34 s at a trapping power of ~ 9 mW. Since inside the RBC, Hb is present in a very high concentration,¹¹ initiation of aggregation by the photoinduced effect may lead to intracellular concentration of Hb beyond the critical supersturation ratio and thus induce rapid polymerization nucleation. Notably, the change in mean Raman signal amplitude [Fig. 7(f)] also follows the heme aggregation pattern. We believe as both

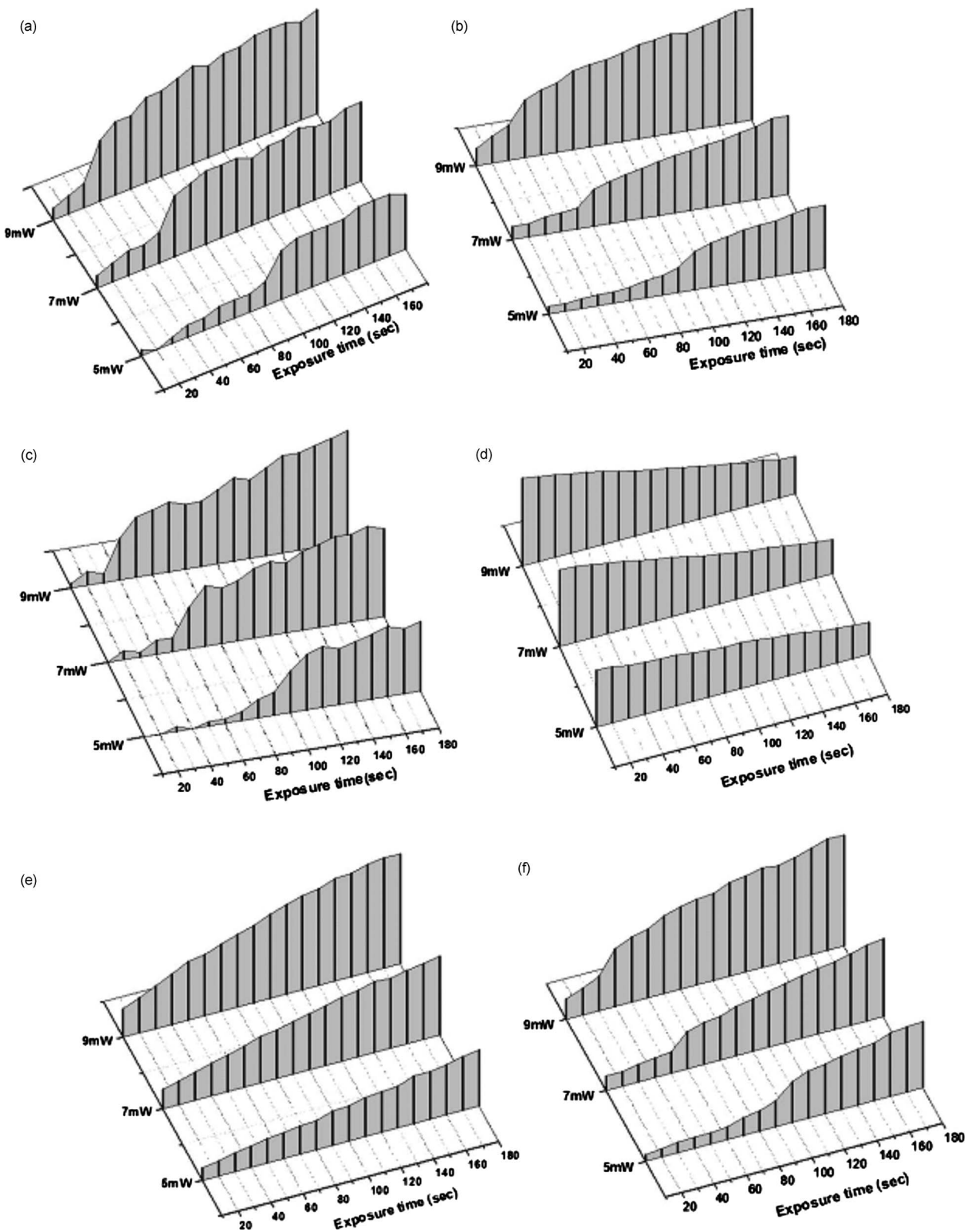


Fig. 7 Temporal variation of relative intensity of Raman bands at (a) 975, (b) 1244, (c) 1366, and (d) 1544 cm^{-1} . The (e) temporal variation of baseline shift in the acquired spectra and (f) the mean Raman signal amplitude are also shown.

elastically and inelastically (Raman scattering) scattered light are expected to be proportional to the number density of the scatterers, therefore, an aggregated cell mass at the laser focus is expected to result in increased Rayleigh scattered and Raman scattered light.

The decrease in intensity of the Raman band at 1544 cm^{-1} [Fig. 7(d)] follows a linear relationship with exposure time. The intensity of this peak is inversely related to the extent of photoinduced hemichrome formation and therefore suggests an increased level of hemichrome with prolonged laser exposure. The hemichrome is known to give strong intrinsic fluorescence that may result in enhanced background in the spectra.³⁰ We noted a similar linear variation for the baseline offsets present in the acquired spectra [Fig. 7(e)].

As discussed earlier, based on the 785-nm-excited micro-Raman spectra of RBC Wood et al.¹² estimated a safe upper limit to be $\sim 18\text{ mW}$. However, results presented in Fig. 7 show that significant photoinduced damage can occur at much lower trap power level ($\sim 5\text{ mW}$) for an acquisition time of $\sim 100\text{ s}$. Note that in contrast to Raman optical tweezers, where cells are optically held in suspension, the cells were fixed on an aluminum-coated Petri dish by poly-L-lysine,¹² which could often result in unwanted surface-induced effects and may also lead to an enhanced background in the acquired spectra, that may mask the small changes that are clearly identifiable in our data.

Note that optical tweezers are increasingly being used for manipulation of different cell types and for manipulation of highly motile cells, such as sperm, and the employment of hundreds of milliwatts of laser power is often necessary. In such studies, it has been shown that cells can be trapped with hundreds of milliwatts of 1064-nm laser power over several minutes without causing significant photodamage.³⁵ The observation of severe photodamage suffered by the RBCs when irradiated with a few milliwatts of 785-nm laser wavelength possibly results from the fact that RBCs have significantly higher light absorption due to a high concentration of intracellular Hb. The molar absorption of oxy-Hb (predominant form of Hb present in the cells studied in our experiments) is $\sim 0.1\text{ mm}^{-1}\text{ mM}^{-1}$, orders of magnitude higher than water (major cellular constituent of the sperm cells) absorption ($0.005\text{ mm}^{-1}\text{ mM}^{-1}$) in this spectral region.^{27,28} Therefore, while the trapping of sperm cells with hundreds of milliwatts of NIR laser power for minutes produces minimum damage, trapping of RBCs using a 785-nm laser results significant damage to the cells. The choice of a 785-nm laser beam for Raman optical tweezers is primarily driven by the facts that at longer wavelengths, the Raman scattering efficiency (vary as $\sim \lambda^{-4}$) is extremely low. For RBCs, using a wavelength of $\sim 785\text{ nm}$ also offers the advantage of resonance enhancement of the Raman spectra.¹² Therefore, use of 780 to 850 nm as the excitation wavelength has become a standard for studying^{7,12,13} Raman spectra of RBCs. This is also aided by the availability of efficient CCD-based detectors at this spectral region.

Note also that for short exposure durations, the recorded Raman spectra suggested normal functionalities of the cells and the observed morphology of the cells in the microscope appears to be normal. Significant photodamage was observed only for longer exposure times ($>30\text{ s}$ at 9 mW to $>90\text{ s}$ at

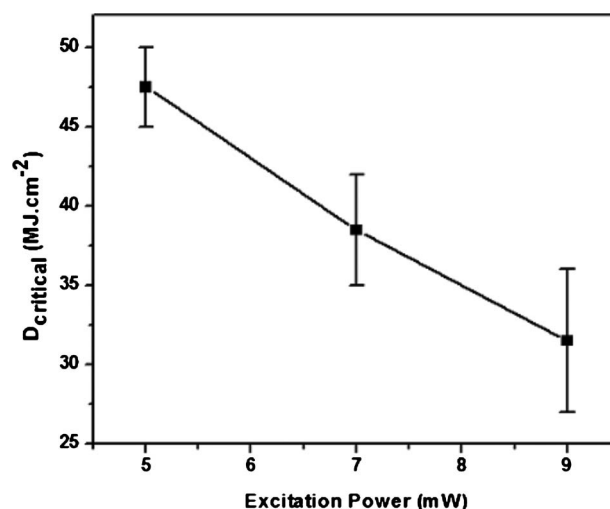


Fig. 8 Accumulated light dosage on RBC at the time of rapid intensity enhancement of Raman bands at 975 , 1244 , and 1366 cm^{-1} .

5 mW). Since for a longer trapping duration, the photodamage resulted to the cells is also consistent over samples collected from different donors, the presence of any predamage in the samples is unlikely.

Figure 8 plots the accumulated light dosage (denoted as D_{critical}) required to observe rapid enhancement of Raman bands associated with a photoinduced aggregation process. The value of D_{critical} estimated for each laser power considering trap spot size is $\sim 0.5\text{ }\mu\text{m}$ for diffraction-limited focusing and the resultant irradiances were ~ 2.55 , ~ 3.57 , and $\sim 4.58\text{ MW cm}^{-2}$ for trapping powers of ~ 5 , ~ 7 , and $\sim 9\text{ mW}$, respectively. The time period for the accumulation of light dosage was estimated from Fig. 7. We can see from Fig. 8 that reduced light dosages are required at higher trapping powers for the initiation of rapid photoaggregation of Hb. This loss of linear reciprocity between laser power and duration of exposure suggests that nonlinear processes may also contribute to the photodegradation of Hb. Such nonlinear absorption is known to take place due to very high light intensity present at the trap focus, even while employing cw NIR sources,³⁶⁻³⁸ where as hemoglobin is known to have very high two-photon absorptivity in the NIR region (780 to 880 nm) with a substantial value³⁹ of $\sim 35\text{ GM}$ at 785 nm. The molecular two-photon absorption rate can be expressed as

$$\phi_{2\text{-ph}} = \sigma_{2\text{-ph}} \left(\frac{P}{\hbar\omega A} \right)^2 N, \quad (3)$$

where $\sigma_{2\text{-ph}}$ is the two-photon absorption cross section for Hb ($\sim 35 \times 10^{-50}\text{ cm}^4\text{ s photon}^{-1}\text{ molecule}^{-1}$), P is the laser power, $\hbar\omega$ is the photon energy, and A is the focal area. The quantity $P/\hbar\omega A$ represents the photon flux density at focus and could be estimated as $\sim 10^{25}\text{ photon cm}^{-2}\text{ s}^{-1}$ for a trapping/excitation power of $\sim 5\text{ mW}$ at 785 nm. The number of Hb molecules present in laser excitation volume N , can be estimated by considering that the mean cellular haemoglobin concentration is ~ 30 to 35 g/dl and the laser excitation volume is limited by the laser spot size and thickness of the

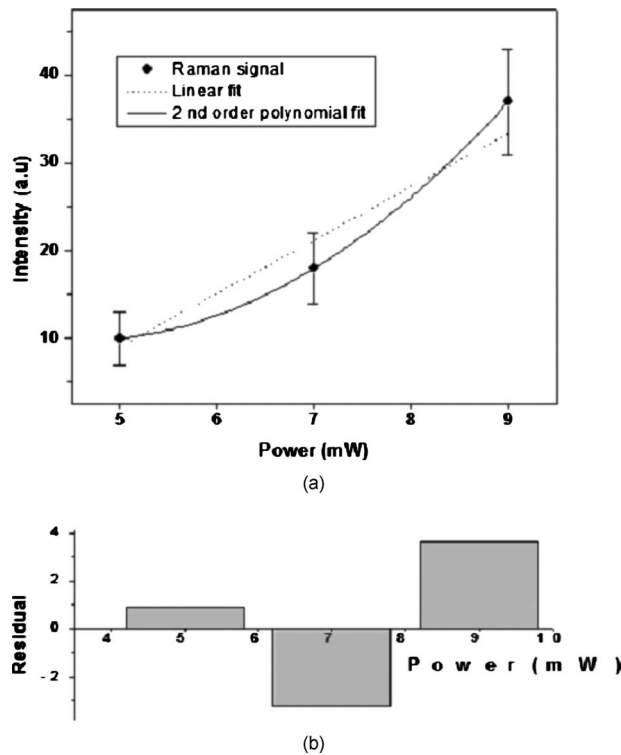


Fig. 9 (a) Change in mean Raman signal amplitude recorded at 25- to 30-s intervals with varying laser power. The solid line shows a second-order polynomial fit and the dashed line shows a linear fit to the data. (b) Residuals for linear fit. Large residual values indicate minimal linear correlation between data.

biconcave RBC ($\sim 2 \mu\text{m}$), as $\sim 10^6$. Therefore a two-photon absorption rate $\Phi_{2\text{-ph}}$ of $\sim 4 \times 10^7 \text{ photons s}^{-1}$ is predicted, which is a modest value.

Figure 9 plots the mean Raman signal amplitude recorded from trapped RBC at 25- 30-s intervals as a function of laser power. The time interval was chosen so that it is at an early point of time before the initiation of any rapid aggregation of intracellular mass (see Fig. 7). From the linear fit and second-order polynomial fit applied to the data, we can clearly see that the variation of intensity is nonlinearly dependent on the excitation laser power. This suggests that as the use of higher laser power leads to higher power density at the beam focus, therefore, an increased two-photon-absorption-induced effect may result, which possibly caused enhanced photodamage to the intracellular Hb.

4 Conclusion

NIR laser excited Raman spectra from optically trapped RBC showed significant photodegradation of hemoglobin even at a nominal excitation/trap power of $\sim 5 \text{ mW}$ for an exposure time beyond 90 s. The results suggest that this is due to photoinduced hemoglobin denaturation and hemichrome formation that eventually leads to hemoglobin aggregation inside the cell.

Acknowledgments

The authors are grateful to M. K. Swami for assistance with the spectrometer and the CCD camera and Dr. D. S. Chitnis, Choithram Hospital and Research Center, Indore, for the blood samples.

References

1. I. R. Lewis and H. G. M. Edwards, *Handbook of Raman Spectroscopy: From the Research Laboratory to the Process Line*, Marcel Dekker, New York (2001).
2. E. Smith and G. Dent, *Modern Raman Spectroscopy—A Practical Approach*, Wiley, New York (2005).
3. D. V. Petrov, "Raman spectroscopy of optically trapped particles," *J. Opt. A, Pure Appl. Opt.* **9**, S139–S156 (2007).
4. 2008 Undergraduate Summer Research Program in Modern Optics and Optical Materials: Detection of nanosize biological threats. Retrieved 3 August, 2008, from University of Arkansas Web site: <http://www.uark.edu/depts/physics/reu05/proj-4.html>.
5. A. Ashkin, "Optical trapping and manipulation of neutral particles using lasers," *Proc. Natl. Acad. Sci. U.S.A.* **94**, 4853–4860 (1997).
6. C. Xie, Y. Li, W. Tang, and R. J. Newton, "Study of dynamical process of heat denaturation in optically trapped single microorganisms by near infra-red Raman spectroscopy," *J. Appl. Phys.* **94**, 6138–6142 (2003).
7. S. Rao, S. Balint, B. Cossins, V. Guallar, and D. V. Petrov, "Raman study of mechanically induced oxygenation state transition of red blood cells using optical tweezers," *Biophys. J.* **96**, 209–216 (2009).
8. C. Xie, D. Chen, and Y. Li, "Raman sorting and identification of single living micro-organisms with optical tweezers," *Opt. Lett.* **30**, 1800–1802 (2005).
9. K. Ramser, K. Logg, M. Goksor, J. Enger, M. Kall, and D. Hanstorp, "Resonance Raman spectroscopy of optically trapped functional erythrocytes," *J. Biomed. Opt.* **9**, 593–600 (2004).
10. K. Ramser, C. Fant, and M. Kall, "Importance of substrate and photo-induced effects in Raman spectroscopy of single functional erythrocytes," *J. Biomed. Opt.* **8**, 173–178 (2003).
11. B. R. Wood, L. Hammer, L. Davis, and D. McNaughton, "Raman microspectroscopy and imaging provides insights into heme aggregation and denaturation within human erythrocytes," *J. Biomed. Opt.* **10**, 014005 (2005).
12. B. R. Wood, P. Caspers, G. J. Puppels, S. Pandiancherri, and D. McNaughton, "Resonance Raman spectroscopy of red blood cells using near infrared excitation," *Anal. Bioanal. Chem.* **387**, 1691–1703 (2007).
13. C. Xie, M. A. Dinno, and Y. Q. Li, "Near-infrared Raman spectroscopy of single optically trapped biological cells," *Opt. Lett.* **27**, 249–251 (2002).
14. A. Trommler, D. Gingell, and H. Wolf, "Red blood cells experience electrostatic repulsion but make molecular adhesions with glass," *Biophys. J.* **48**, 835–841 (1985).
15. A. Rossi-Fanelli, E. Antonini, and A. Caputo, "Studies on the relations between molecular and functional properties of hemoglobin," *J. Biol. Chem.* **236**, 391–396 (1961).
16. A. K. Sau, D. Currell, S. Mazumdar, and S. Mitra, "Interaction of sodium dodecyl sulfate with human native and cross-linked hemoglobins: a transient kinetic study," *Biophys. Chem.* **98**, 267–273 (2002).
17. F. Roux-Dalvai, A. Gonzalez de Peredo, C. Simó, L. Guerrier, D. Bouyssié, A. Zanella, A. Citterio, O. Burllet-Schiltz, E. Boschetti, P. Giorgio Righetti, and B. Monsarrat, "Extensive analysis of the cytoplasmic proteome of human erythrocytes using the peptide ligand library technology and advanced mass spectrometry," *Mol. Cell Proteomics* **7**, 2254–2269 (2008).
18. B. R. Wood, B. Tait, and D. McNaughton, "Micro-Raman characterization of the R to T state transition of haemoglobin within a single living erythrocyte," *Biochim. Biophys. Acta* **1539**, 58–70 (2001).
19. M. Abe, T. Kitagawa, and Y. Kyogoku, "Resonance Raman spectra of octaethylporphyrinato-Ni(II) and meso-deuterated and 15N substituted derivatives. II. A normal coordinate analysis," *J. Chem. Phys.* **69**, 4526–4534 (1978).
20. S. Hu, K. M. Smith, and T. G. Spiro, "Assignment of protoheme resonance Raman spectrum by heme labeling in myoglobin," *J. Am. Chem. Soc.* **118**, 12638–12646 (1996).
21. B. R. Wood and D. McNaughton, "Raman excitation wavelength in-

- vestigation of single red blood cells *in vivo*," *J. Raman Spectrosc.* **33**, 517–523 (2002).
22. M. Asghari-Khiavi, A. Mechler, K. R. Bambery, D. McNaughton, and B. R. Wood, "A resonance Raman spectroscopic investigation into the effects of fixation and dehydration on heme environment of hemoglobin," *J. Raman Spectrosc.* **40**, 1668–1674 (2009).
 23. A. C. De Luca, G. Rusciano, R. Ciancia, V. Martinelli, G. Pesce, B. Rotoli, L. Selvaggi, and A. Sasso, "Spectroscopical and mechanical characterization of normal and thalassemic red blood cells by Raman tweezers," *Opt. Express* **16**, 7943–7957 (2008).
 24. M. Asghari-Khiavi, B. R. Wood, A. Mechler, K. R. Bambery, D. W. Buckingham, B. M. Cookec, and D. McNaughton, "Correlation of atomic force microscopy and Raman microspectroscopy to study the effects of *ex vivo* treatment procedures on human red blood cells," *Analyst (Amsterdam)* **135**, 525–530 (2010).
 25. L. R. Moore, H. Fujioka, P. S. Williams, J. J. Chalmers, B. Grimberg, P. A. Zimmerman, and M. Zborowski, "Hemoglobin degradation in malaria-infected erythrocytes determined from live cell magnetophoresis," *FASEB J.* **20**, 747–749 (2006).
 26. E. J. G. Peterman, F. Gittes, and C. F. Schmidt, "Laser-induced heating in optical traps," *Biophys. J.* **84**, 1308–1316 (2003).
 27. R. C. Smith and K. S. Baker, "Optical properties of the clearest natural waters (200–800 nm)," *Appl. Opt.* **20**, 177–184 (1981).
 28. S. Prahl, "Optical absorption of haemoglobin," Oregon Medical Laser Center, retrieved Feb. 5, 2010, from http://www.imt.liu.se/edu/courses/TBMT36/artiklar/4_Tissue_prop/hemoglobin_spectra.pdf.
 29. V. M. Nahirnyak, S. Wang Yoon, and C. K. Holland, "Acoustomechanical and thermal properties of clotted blood," *J. Acoust. Soc. Am.* **119**, 3766–3772 (2007).
 30. S. C. M. Agostinho, M. H. Tinto, J. R. Perussi, M. Tabak, and H. Imasato, "Fluorescence studies of extracellular hemoglobin of *Glossoscolex paulistus* in Met form obtained from Sephadex gel filtration—a natural deconvolution of circular dichroism curves of proteins," *Comp. Biochem. Physiol. A* **118**, 171–181 (1997).
 31. S. K. Mohanty, A. Uppal, and P. K. Gupta, "Self-rotation of red blood cells in optical tweezers: prospects for high throughput malaria diagnosis," *Biotechnol. Lett.* **26**, 971–974 (2004).
 32. S. K. Mohanty, K. S. Mohanty, and P. K. Gupta, "Dynamics of interaction of RBC with optical tweezers," *Opt. Express* **13**, 4745–4751 (2005).
 33. S. Grover, R. Gauthier, and A. Skirtach "Analysis of the behaviour of erythrocytes in an optical trapping system," *Opt. Express* **7**, 533–539 (2000).
 34. M. Zhou, H. Yang, J. Di, and E. Zhao, "Manipulation on human red blood cells with femtosecond optical tweezers," *Chin. Opt. Lett.* **6**, 919–921 (2008).
 35. J. M. Nascimento, E. L. Botvinick, L. Z. Shi, B. Durrant, and M. W. Berns, "Analysis of sperm motility using optical tweezers," *J. Biomed. Opt.* **11**, 044001 (2006).
 36. Y. Liu, G. J. Sonek, M. W. Berns, K. König, and B. J. Tromberg, "Two-photon fluorescence excitation in continuous-wave infrared optical tweezers," *Opt. Lett.* **20**, 2246–2248 (1995).
 37. S. W. Hell, M. Booth, S. Wilms, C. M. Schmetter, A. K. Kirsch, D. J. Arndt-Jovin, and T. M. Jovin, "Two-photon near- and far-field fluorescence microscopy with continuous-wave excitation," *Opt. Lett.* **23**, 1238–1240 (1998).
 38. K. König, H. Liang, M. W. Berns, and B. J. Tromberg, "Cell damage in near-infrared multimode optical traps as a result of multiphoton absorption," *Opt. Lett.* **21**, 1090–1092 (1996).
 39. G. O. Clay, C. B. Schaffer, and D. Kleinfeld, "Large two-photon absorptivity of hemoglobin in the infrared range of 780–880 nm," *J. Chem. Phys.* **126**, 025102 (2007).